HKIE THE HONG KONG INSTITUTION OF ENGINEERS 香港工程師學會

AI-powered inspections of facades in reinforced concrete buildings

Michele De Filippo[1], Sasan Asadiabadi[1], J S Kuang[2], Dhanada K Mishra[1] and Harris Sun[1]

[1] RaSpect Intelligence Inspection Limited, Hong Kong, People's Republic of China
[2] Department of Civil and Environmental Engineering, The Hong Kong University of Science and Technology, Hong Kong, People's Republic of China

ABSTRACT

Worldwide there are plenty of aged Reinforced Concrete (RC) buildings in need of thorough inspections. Cracks, delamination, stains, leakages, debonding and moisture ingressions are common defects found in RC structures. Such problems are typically diagnosed through qualitative assessment of visual and thermal photographs (data) by certified inspectors. However, qualitative inspections are very tedious, time-consuming and costly. This paper presents an alternative novel approach to drastically increase efficiency by decreasing the data collection and analysis time. Data collection for the inspection of facades is undertaken with Unmanned Aerial Vehicles (UAVs) either through an autonomous pre-programmed flight or through a human-piloted flight. Data analysis is performed by implementing up-to-date AI-powered algorithms to automatically detect defects on visual and thermal photographs. All the recognised defects and thermal anomalies are labelled on the building facade for comprehensive evaluation of the asset. This paper reports that the implementation of AI-powered inspections can save up to 67% of the time spent and 52% of the cost in comparison to the most commonly adopted practice in the industry with an average accuracy of 90.5% and 82% for detection of visual defects and thermal anomalies, respectively.

KEYWORDS AI; civil engineering; computer vision; crack; deep learning; leakage; reinforced concrete; thermography; UAV
CONTACT Michele De Filippo michele.defilippo@alumni.ust.hk
Received 27 March 2020

1. Introduction

In Hong Kong, there is a great abundance of aged buildings and infrastructure for which an assessment of their current status is needed (Kwan and Wong, 2005). In 2017, a balcony of a subdivided flat in a 60-year-old tenement building collapsed. Miraculously the catastrophe did not cause any casualties (Zhao, 2017). Such an accident recalls to the memory two similar incidents, in 2010 and in 2013, when buildings aged 50+ years old collapsed, killing a total of four residents and leaving dozens homeless (Zhao, 2017). Several accidents of sudden failures have occurred throughout the past decade, causing financial losses, physical damage to infrastructure, goods, and, most importantly, casualties. The city has increasingly dangerous maintenance and subdivision problems with old buildings, where owners often cannot afford their upkeep. The aforementioned tragedies led to the Mandatory Building Inspection Scheme (MBIS) (Building Department, 2012), which came into force in 2012, despite owners' complaints about the cost and inconvenience.

According to the current Hong Kong legislation, under the MBIS, owners of buildings aged 30 years or above must undergo inspections once every ten years. Repetitive 10-yearly inspections for buildings aged 30+ years old are demanding in terms of both time and cost. It is estimated by the Building Department that in Hong Kong, there are 40,758 privately owned buildings, and a consistent number of them are 30+ years old, precisely about 21,929, corresponding to 53.8% of all privately owned buildings (see Table 1) (Mavromatidis et al., 2014). The difficulties constraining periodic inspections of old private buildings are mainly cost and time, resulting in unsuccessful MBIS legislature (Corsi, 2010; Harvey et al., 2016).

Table 1. Age of existing privately-owned buildings.

Construction period		Amount of existing privately-owned buildings	
from	to		
1900	1909	4	≥ 30 years old
1910	1919	1	
1920	1929	1	
1930	1939	7	
1940	1949	313	
1950	1959	1,876	
1960	1969	5,133	
1970	1979	5,936	
1980	1989	8,658	
1990	1999	8,642	< 30 years old
2000	2009	2,433	
2010	2019	921	

Given the large number of buildings needing inspections and the necessity of inspections on a 10-year basis, an automated and scalable solution would be greatly beneficial for the building inspection industry.

The method proposed in this paper fills these gaps by providing a solution for automated AI-powered building inspections. Besides the highlighted legal necessity of inspections, the proposed method also tackles the following problems:

- Lack of an established understanding of the degree of structural deterioration in common residential buildings
- Lack of information on the satisfaction level of building owners regarding the current status of their assets
- Lack of understanding of the life expectancy and risks related to existing buildings

2. Motivation

Methodologies for building inspections can be segmented into two main categories: qualitative and quantitative approaches.

2.1. Qualitative approach

A qualitative approach is mainly based on non-numerical information. Qualitative analyses are interpretative; hence, they may be subjective. When it comes to inspecting buildings, a qualitative approach requires manpower from professionally certified inspectors and provides an in-depth description. In the past few decades, qualitative methods have been extensively used for building inspections, and nowadays, they are still the most widespread yet accurate methodology. Given the large amount of existing degrading structures and the afore-mentioned increasingly frequent sudden collapses, inspections are needed to ensure that existing buildings are maintained in a safe state. Canonical inspections require prior setting up of scaffoldings or gondolas along with human labour to carry out the inspections. The main drawbacks are the extensive necessity for manpower, time and cost; hence, qualitative approaches are hardly scalable to densely populated cities, such as Hong Kong.

2.2. Quantitative approach

Quantitative approaches represent a valid alternative to qualitative approaches. The usage of a quantitative approach is useful for tackling the problem of the inspection of buildings through fast collection and automated processing of extracted numerical data. AI-powered technology can be used for automating and speeding up the inspection process. Through such an approach, a multitude of information is extracted in an automated manner from visual and thermal photographs taken with UAVs. Subsequently, they are processed by AI engines including Deep Learning (DL) algorithms for defect detection in visual data and a Computer Vision (CV) algorithm for anomaly detection based on thermal data. The idea is that an 'AI-powered diagnosis' of buildings is performed according to the detection of certain categories of defects duly selected and stored in a database.

The processes involved in the proposed methodology, including data collection and analysis, are given in the following sections.

3. Data collection

Visual and thermal cameras mounted on UAVs enable professionals to collect visual and thermal photographs (data) of building facades efficiently and accurately, thereby reducing operational costs and safety risks. UAVs provide building inspectors with a unique aerial perspective. Drones allow easy access to remote or inaccessible areas (which may include natural or human-built obstructions) without compromising safety (Mavromatidis et al., 2014). Compared to traditional inspection methods, the use of UAVs increases the quality of the collected data and allows for repetitive data collection in the monitoring of historical or structurally damaged buildings (Clark et al., 2003; Corsi, 2010; Harvey et al., 2016). Another benefit of utilising UAVs for building inspections is the non-destructive and non-contact approach (Barreira and Freitas, 2007; Mercuri et al., 2014). Accordingly inspections are performed by employing a drone equipped with a visual and thermal camera to conduct rapid surveys of building facades.

3.1. Flight-path design

Whilst UAVs are starting to be employed in building inspection activities, a comprehensive common ground for UAV building inspection procedures has not yet been established. Rakha et al. (Rakha and Gorodetsky, 2018) compared research studies on recommended ideal flight distances for facade inspection, as reported in Figure 1. Among the different strategies mentioned by Rakha et al., the authors adopted the procedure highlighted in Figure 2 and the recommendations given in Section 3.2. The flight path can either be remotely controlled by a pilot or pre-programmed using third-party software (Flylitchi, 2020).

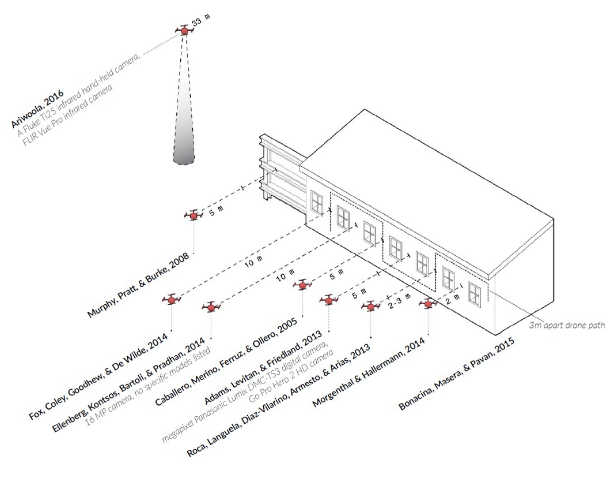

Figure 1. Drone inspection distances as reported in the literature on the surveying in facade and building inspection (Rakha and Gorodetsky, 2018).

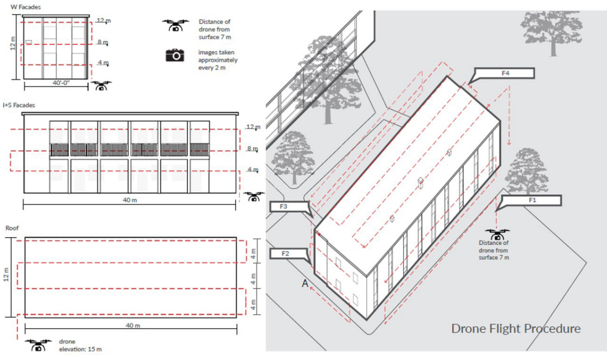

Figure 2. Drone flight procedure for the surveying in facade and building inspection (Rakha et al., 2018).

3.2. Recommendations for data collection

The analytics, to be presented in the following sections, have been designed to analyse visual and thermal data in conformance with the following specifications:

- Outdoor environmental conditions must be measured, and it has to be determined if the climate is suitable for performing a flight (temperature, humidity, wind speed, cloud coverage, etc.).
- The indoor temperature must be measured (or assumed) and the resulting temperature difference has to be calculated. It has to be determined whether the difference is within the acceptable range (10°C or more).
- Building usage (building type, operating hours, etc.) must be determined.
- Occupants must be notified of the flight, and they must be asked to minimise radio and Wi-Fi interference.
- For flat facades that are mostly vertical, the flight path should begin on a predetermined corner and follow vertical bays upward, move across to the next bay, and proceed downward. This pattern is repeated until the entire facade has been documented, and the drone moves on to the next facade in a similar manner. For flat facades that are mostly horizontal, the path should begin at a predetermined corner and continue to the right before moving up a bay and continuing in a linear manner to the left, repeating this until the entire facade has been documented. After capturing facades, the drone should capture images of the roof in a similar grid manner, starting from one corner and moving in either a horizontal or vertical pattern along a superimposed grid until the entire roof has been captured (see Figure 2).
- Minimum image resolution should be 640x480.
- Photos should have 70-80% overlap.
- The UAV should be at a distance of ~3-7 m from the facade, depending on the inspection site and building type.
- During the inspection, the pilot should keep the camera in such a way that the projection of the camera on the facade is always orthogonal.
- The subject being inspected should always be in clear focus at a fixed distance.
- The data should not include any object lying at a distance between the facade being inspected and the camera.
- Ideally, the data should not include regions not undergoing thermal inspection such as sky, clouds, neighbouring buildings, people, trees, etc.
- It is important to note that visual and thermal data are sensitive to weather conditions. Climatic factors such as rain, heavy wind and snow can considerably affect the outcome of an inspection. Other environmental factors, such as solar radiation, cloud coverage, wind speed and humidity, can affect the visibility and the external surface temperature. Through a series of test flights and literature studies, Entrop and Vasenev (2017) developed a protocol for the usage of UAVs for thermal inspections. Such additional recommendations are followed to ensure a high quality of collected data.

4. Visual analytics

To automate the inspection of defects on RC structures, throughout the past few years various automated robotic-based systems have been studied. Pereira and Eduardo (2015) were among the first to propose using UAVs and visual photographs for the autonomous inspection of building cracks. Their study compares different CV-based algorithms and evaluates their performances in many aspects, including the runtime on different platforms, binary size, and code complexity. Oh et al. (2009) developed an early visual inspection vehicle robot that used batch processes for crack detection. Khan et al. (2015) implemented vision-based UAV robots for bridge inspection and condition assessment, in which conventional image processing approaches were applied for crack identification. In the manufacturing industry, AI-powered inspection has already found many applications (Kim et al., 2021; Nwankpa et al., 2021). Perez et al. (2019) presented a deep learning approach for detecting building defects using a Convolutional Neural Network (CNN). Using UAV data, Garcia de Soto (2021) developed a model an automated building inspection for cracks.

Based on previous research on non-destructive evaluation for concrete inspection, it is very promising to deploy UAV inspection for low-cost and omni-bearing detection. However, nowadays, there is still a lack of an automated procedure for thoroughly replacing the qualitative approaches described in Section 2.1 for visual inspections. Herein, the authors propose an approach for defect classification powered by Deep Learning (DL) based on visual data, herein referred to as 'Visual Analytics'. The visual analytics workflow is described as follows.

4.1. Visual analytics workflow

A method for the detection and analysis of architectural defects of facades is proposed. The algorithm is structured in a two-stage scheme: (1) Macro inspection, in which the defects in the image are localised using a Deep Neural Network (DNN) and (2) Micro inspection, in which the localised defects from stage (1) are analysed to assess their severity.

In the following, the steps taken to develop the method are discussed.

4.2. Data preparation and labelling

After research studies and analysis of inspection demand within the industry, the authors have identified cracks, delamination, and stain as the structural defects more likely to be visible on the facades of RC buildings in Hong Kong. A crucial factor for training a DNN is the availability of enough annotated data so that the model can successfully learn features from the inputs. Due to a shortage of existing publicly available datasets on local Hong Kong architecture, the authors collected a training dataset for defect detection. The data were collected according to the specification given in Section 3 for five RC buildings. Data labelling is a tedious and time-consuming process requiring civil engineering specialists to analyse the dataset manually (Chen et al., 2019). A civil engineer has annotated the collected images, using a bounding box label around defects in the image. Figure 3 illustrates an example of an annotated image from the training dataset. In total, the training dataset for macro inspection is comprehensive with 650 images of the size 4056x3040. The VIA annotation tool (Dutta and Zisserman, 2019; Dutta et al., 2016) is used to perform the data annotation.

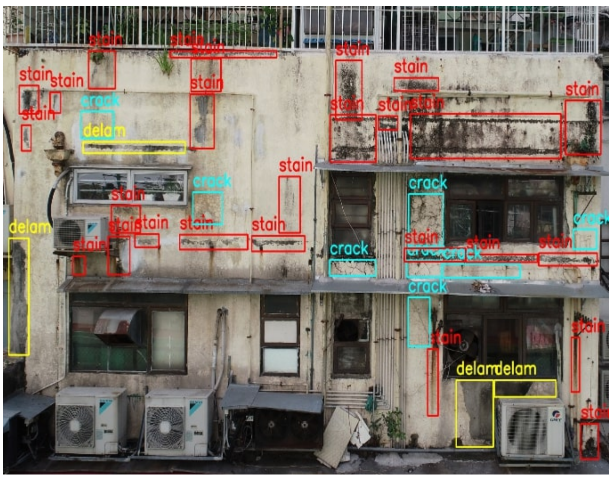

Figure 3. Snapshot of a sample annotated image from the training dataset for macro inspection.

For micro inspection, data annotation becomes even more tedious. Annotation has to be performed pixel-wise, namely all pixels have to be annotated as belonging or not belonging to a defect. The micro inspection training dataset is comprehensive in regard to the collected data used for macro inspection and publicly available images from the web. The performed web search used the following keywords:

- For concrete crack: Concrete crack, crack repair, concrete separation, concrete scaling, concrete crazing, etc. yielded a total of 18,126 images, and 722 images were used for crack detection.
- For concrete delamination: Concrete spalling, concrete delamination, concrete facade spalling, concrete column spalling, concrete spalling from fire, concrete spalling repair, concrete wall, etc. yielded a total of 22,268 images, and 532 were used for delamination detection.
- For concrete stain: Concrete stain, concrete water-based stain, concrete aberration, concrete anomalous pigments, concrete discolours, etc. yielded a total of 19,272 images, and 513 were used for stain detection.

The 722 crack images, 532 delamination images and 513 stain images made up the initial training database. Since the randomly posted images on the web are not well tagged with the flaw area, and the shape of the defect region tends to be stochastic in distribution, it is necessary for areas to be manually labelled as shown in Figure 4.

(a)

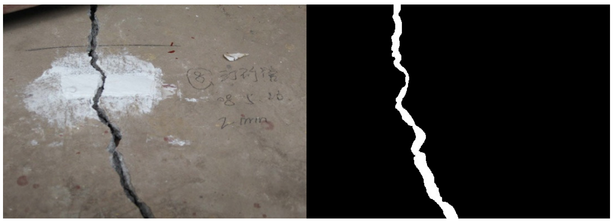

(b)

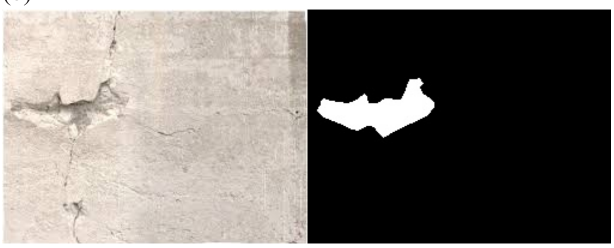

(c)

Figure 4. Data labelling for the micro inspection of (a) cracks; (b) delamination; and (c) stains.

4.3. Macro inspection

Macro inspection is performed through a fine-tuned RetinaNET-based object detector (Abadi et al., 2014; Abadi et al., 2016). The RetinaNet model takes an image as the input and detects the desired objects via finding a bounding box around the object and assigns a class label to each. A representation of the network architecture is presented in Figure 5. The network utilises a ResNet50 architecture as the backbone to extract high-definition image features for the supervised learning task. The input image is analysed at different scales through a Feature Pyramid Network (FPN), which supports the detection of objects of various sizes. Feature maps at different scales are then blended to perform the object detection task.

A pre-trained ResNet50 is utilised at the network's backbone to speed up the model convergence process during training. The pre-trained weights are used to initialise the model. The backbone weights are frozen for the first 15 epochs, and only the network head's parameters are optimised to train the network. The head's parameters are used for bounding box regression and prediction of class probability. After the 15th epoch, all the network parameters are optimised using an Adam optimizer (Kingma and Ba, 2014). The network is trained for 200 epochs with a batch size of 4, with early stopping enabled to terminate the training in the case of no loss improvement. The initial learning rate in Adam is set to 1-5, and an adaptive learning rate scheduler is set to further reduce the loss.

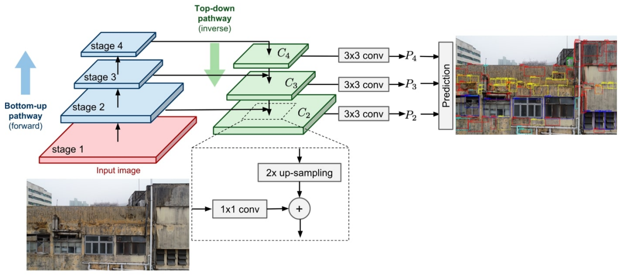

Figure 5. RetinaNet Architecture implemented for defect detection in the macro inspection stage. The network receives an RBG image at the input and detects the location and labels the defects at the output.

4.4. Micro inspection and defect assessment

Micro inspection is performed using a Fully Convolutional Network (FCN) based on object segmentation (Chen et al., 2019) to assess the severity of detected defects from macro inspection. An FCN receives the defect images (delimited by bounding boxes), resizes defects to a 224x224 resolution, and produces a binary output image. The output binary is represented as a matrix of pixels with values of 255 at the defect locations and 0 otherwise. This binary image is then utilised to analyse the defect attributes within each detected bounding box. An FCN-8 object segmentor (Long et al., 2014) generates the binarised targets from the input RBG images. FCN-8 utilises a VGG16 network (Simonyan and Zisserman, 2014) at the encoder to generate features discriminating the desired object from the background. The feature maps at different levels are then up-sampled and blended to generate the segmented output image at the decoder part. An FCN is trained separately for each defect class. Figure 6 illustrates the details of the FCN-8 network architecture.

A pre-trained VGG16 model is utilised in the encoder stage of the network. The network is trained to minimise the Mean Squared Error (MSE) Loss on the output binary images. The Adam optimizer is used to optimise the parameters of the network. The network is trained for 50 epochs with a batch size of 32, with early stopping enabled to terminate the training in the case of no loss improvement. The initial learning rate in Adam is set to 1-5, and an adaptive learning rate scheduler is set to reduce the loss further.

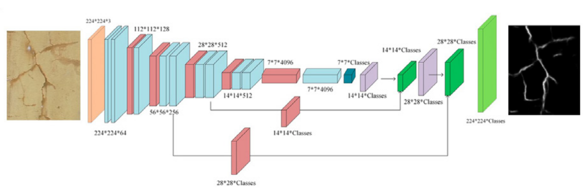

Figure 6. FCN-based micro-inspection model. The network receives an RBG image at the input and generates the segmented output.

All networks related to the macro and micro inspection are implemented in Keras (Chollet, 2015) using TensorFlow backend (Abadi et al., 2016) on an NVIDIA TITAN XP GPU.

The assessment of defects in the form of cracks, delamination and stain quantification is performed by assigning several attributes to each defect class, using the results from the micro inspection. Such attributes, including crack width and the defect area to bounding box ratio, are used to assess the severity of each defect in conformance with earlier work (Arena et al., 2014; Kim et al., 2017), and to categorise their severity level as 'minor', 'medium' or 'severe'. The basis of severity for cracks (Bauer et al., 2017), delamination (Shamsudin et al., 2017) and stain (Buildings Department, 2012) classes are reported in Table 2 below.

Table 2. Criteria for micro-inspection labelling of defects.

Defect class	Minor	Medium	Severe
Cracks	Hairline and fine cracks: 0.1 mm < w < 1 mm	Cracks: 1 mm < w < 15 mm	Extensive or structural cracks: 15 mm < w
Delamination	Delaminated area < 150 mm in any direction	Delaminated area: 150-300 mm in any direction	Delaminated area > 300 mm in any direction
Stain	Area < 0.1 m^2	Area: 0.1 m2 < A < 1.0 m^2	Area: A > 1.0 m^2

4.5. Post-processing and labelling of defects

The dataset is split into training and testing datasets in the proportion of 70% and 30%, respectively. After the model is trained on the training data, it can be used for defect classification detection. For a constant sub-image size, a sliding window is used to perform detection throughout the entire image. Then at the inference level, the model labels classes in each image along with the respective severity. After training on the initial dataset, the model is tested, the detection results are manually reviewed, and final decisions are made. The reviewed labelled images are used for re-training purposes, and the model benefits from this feedback loop with constant improvements in performance inspection after inspection. Figure 7 shows a sample application of visual analytics through macro inspection and micro inspection on the facade of an RC building. It is noted that besides training for defect classification, as mentioned in Section 4.2, training data also include labels of other elements typically present in the Hong Kong architecture of RC buildings, such as windows and air conditioners. The displayed results are representative of the overall accuracy of macro inspection.

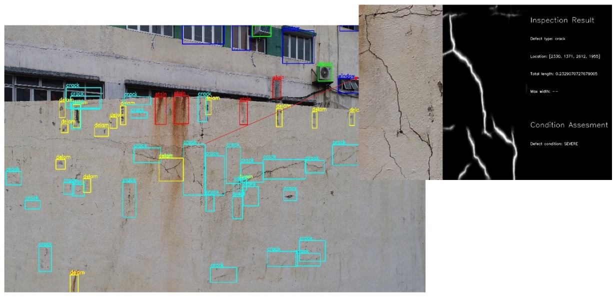

Figure 7. Sample illustration of the application for visual analytics.

The abovementioned process of labelling and re-training has been undertaken through several inspections, and the database has been extended to 18,000+ labelled images. The model's accuracy is benchmarked against the test data, and the result is reported in Figure 8. The metric used for accuracy is the F1-score. From the figure, it can be noticed that accuracy in regard to window and air conditioner detection is much greater than for defect detection. Such a result is attributed to the fact that windows and air conditioners have more articulated and distinctive features than defects; hence, their detection represents a less complex CV problem. Regarding the accuracy of defects, the difference is attributed to data availability in the dataset, which is partitioned with 40% cracks labels, 27% delamination labels and 33% stain labels. Additionally, delamination and stains can in some cases be misdetected due to their similar distinctive features such as colour and shape.

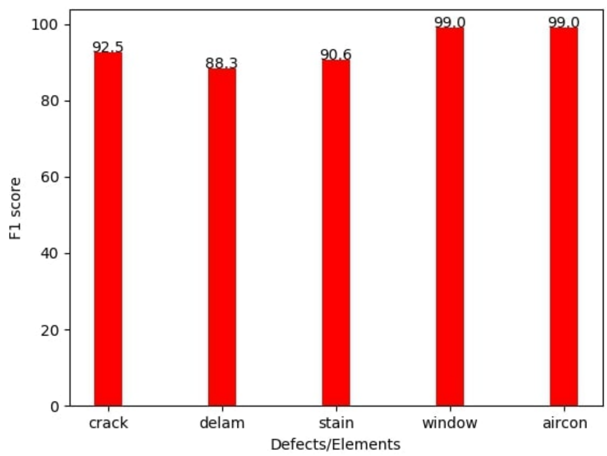

Figure 8. Achieved accuracy for visual analytics.

5. Infrared analytics

To automate the detection of thermal anomalies in thermal photographs, several approaches have been studied. A research work on automated detection of thermal heat losses in the proximity of windows was proposed by Martinez-De Dios and Ollero (2006). It was proposed to track heat-loss areas according to a fixed threshold of 7°C. However, such an approach may be prone to infeasibility and errors according to weather conditions and building materials. Zhang et al. (2015) presented a method for thermal inspection of roofs using UAVs to facilitate both visual interpretation and autonomous detection. The investigation used Markov Random Fields on superpixels to segment the anomalous regions of the thermal image. A more comprehensive approach utilising thermographic automation was introduced by Mauriello and Froehlich (2014). In a later research paper, Mauriello et al. highlighted the challenges and problems related to automation, data quality, and technical feasibility (Mauriello et al., 2015). The most recent updates on thermal inspections are provided by Rakha et al. (2018), who presented a methodology for employing drones to conduct thermal building inspections with UAVs.

Based on the past research on non-destructive evaluation for concrete inspection, it is very promising to deploy UAV inspection for thermal anomaly detection. However, nowadays, there is still a lack of a reliable and automated procedure for replacing qualitative approaches described in Section 2.1 for thermal inspections. By collecting an increasing amount of data along with corresponding spatial information, data-driven classification and recognition approaches based on CV show the potential to provide more solid and scalable inspection results compared to conventional approaches.

In this paper, the authors propose an approach for CV-based anomaly detection based on thermal data, herein referred to as 'infrared analytics'. In such an approach, thermal anomalies are detected in an automated manner and diagnosis of thermal anomalies is undertaken in the post-processing phase to assess the causes. A comprehensive description of the infrared analytics workflow is described as follows.

5.1. Infrared analytics workflow

A method to detect and analyse anomalies in a thermal image is proposed. Similar to the visual analytics procedure covered previously (see Section 4.1), the infrared analytics algorithm is structured in a two-stage scheme: (1) macro inspection, in which the thermal anomalies are detected using a CV-based algorithm (De Filippo et al., 2019) and (2) micro inspection, in which the localised anomalies from stage (1) are analysed to assess the severity of anomalies. In the following, the steps taken to develop the method are discussed.

5.2. Data preparation

After research studies and analysis of inspection demand within the industry, the authors have identified leakage, debonding and moisture as target thermal defects in RC facades. It should be noted that, similar to the data collection for visual analytics (see Section 4.2), a web keyword search for such structural defects provides non-optimal results. Accordingly, finding online sources for thermal photographs is challenging. Thermal data were collected simultaneously with visual data for the same five RC buildings mentioned in Section 4.2. The database used for development of the algorithm being described consists of the following:

- For leakage: A total of 325 images were collected.
- For debonding: A total of 203 images were collected.
- For moisture: A total of 289 images were collected.

The 325 leakage images, 203 debonding images and 289 moisture images made up the initial database. Since the randomly posted images on the web are not well tagged with the flaw area, and the shape of the defect region tends to be stochastic in distribution, it is necessary for areas to be manually labelled. Data labelling of thermal images is a very tedious and time-consuming process that requires the employment of infrared civil engineering specialists to analyse the above-mentioned dataset manually (De Filippo et al., 2019).

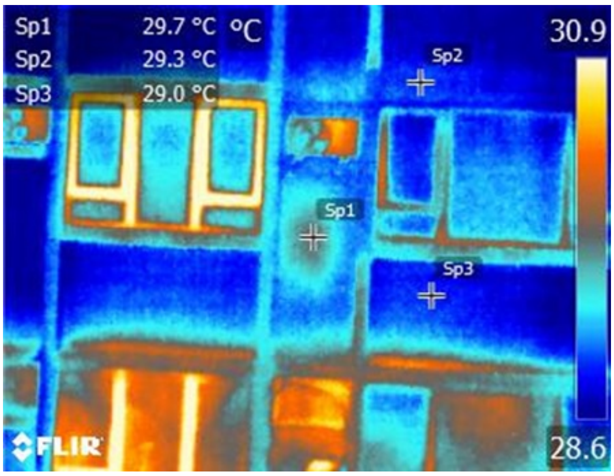

Figure 9. Snapshot of a sample annotated infrared image from the training dataset for macro inspection with sp1 being leakage, and sp2 and sp3 being moisture.

5.3. Macro inspection

A thermal anomaly is defined as a region where sharp and abnormal temperature changes occur in the thermal image. The macro inspection algorithm is designed for the detection of thermal anomalies. In this framework, a thermal image is considered as a two-dimensional matrix, whose cells (pixels) are temperature values. A naïve solution to segment the anomalous regions would be looking for sufficiently cold pixels (in summer, for outdoor images) and labelling them as anomalous. However, this approach can lead to multiple false-positive results since such pixel-wise separation works as a simple filter detecting cold regions without taking any distinctive characteristic of thermal anomalies into account. Sharp temperature changes are delimited by thermal edges, hence representing the contour of anomalous regions. It can be inferred that thermal anomalies are regions bounded by thermal edges. Yet, the data may contain other non-relevant visible edges that will be detected on the same image which do not bound any thermal anomalies (e.g., trees, clouds, etc.). To address this challenge, the proposed method segments out anomalous regions through thermal edges, and applies thermal anomaly segmentation to the remaining regions. The algorithm for macro inspection is composed of 'Dynamic Calibration and Identification of Thermal Edges and Anomaly Segmentation', which is introduced as follows.

5.3.1. Dynamic calibration

The first stage of the algorithm outputs two thresholds calculated per image based on the temperature distribution and seasonal conditions. Instead of defining a strict, pre-set threshold, the algorithm finds appropriate thresholds for each image before further processing. These two thresholds are referred to as Anomaly Threshold (AT) and Bin Width (BW). The AT is used to determine which pixels are anomaly candidates, while the BW is used to assess if temperature change is happening in a certain region. They are computed by employing a temperature histogram, whose size is dynamic based on the representativeness of the histogram bins (see Figure 10). The Anomaly Bins (AB) are defined as the bins where anomalous pixel values fall, and they lie behind the AT. The Opposite Bin (OB) is defined as the bin at the opposite side of the AB associated with the greatest temperature values. To eliminate some of the false-positives, a lower α limit is used as the representativeness of the OB since the expectation is for it to contain enough values. If the OB contains less than α, the values that fall into it are removed, and the histogram is recalculated until the OB has strong representativeness.

It is assumed that if there is more than one peak in the histogram, then the pixel distribution may contain irrelevant information leading to false positives (such as background sky). In such a case, the relevant information is likely at mid-range temperatures. Eventual irrelevant peaks and their bounding pixels are discarded.

Next, an upper β limit is used on the AB, which is not expected to dominate the temperature distribution since the total area of potential anomalous regions is likely to occupy a smaller portion of the entire image. If the representativeness of the AB is greater than β, the number of bins is incremented and recomputed until the limiting condition is met. The abovementioned α and β limits are variable percentage values tuned according to the thermal data distribution depending on the building type.

(a)

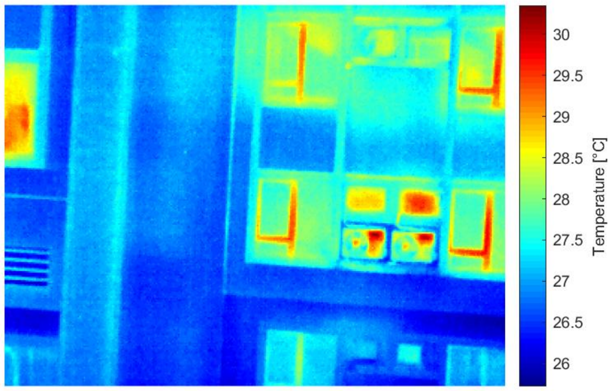

(b)

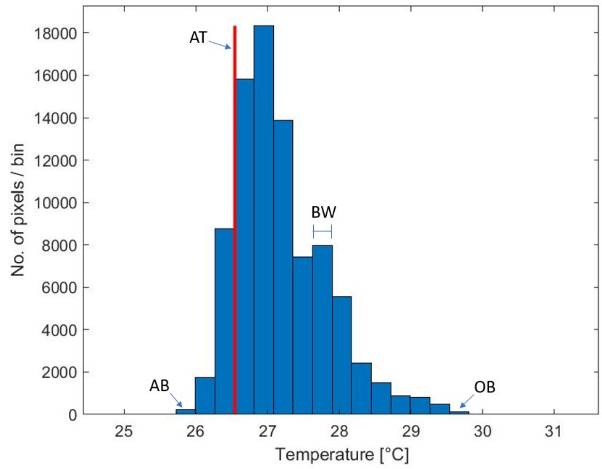

Figure 10. (a) Sample thermal image; and (b) histogram of thermal data.

5.3.2. Identification of thermal edges and anomaly segmentation

In the second stage of the algorithm, the thermal edges are found by using a Canny edge detector (Canny, 1986). By utilising the thresholds that were established earlier, the irrelevant edges generated by the Canny edge detector are filtered out. The filtering operation is done by processing every pixel on each edge line along the edge direction and judging if they are pixels on the edge of a thermal anomaly or not. During this process, the algorithm compares the values in the neighbourhood of the pixel currently being processed. A neighbourhood relationship is established, with the neighbourhood defined as a set of values perpendicular to the edge direction (De Filippo and Kuang, 2021). If the greatest value in the neighbourhood is greater than the AT (that is, the corresponding pixel does not fall in the AB), the corresponding edge pixel is removed. If it is lesser than the AT, the algorithm checks whether the difference between the highest and lowest values is larger than the BW. If the difference is not larger, the current edge pixel is removed. Otherwise, the algorithm keeps the edge pixel and moves on to the next one. Anomalous edges are found after processing all pixels on each edge and performing elimination. As a result, the actual anomalous regions enclosed by these edges are highlighted by a bounding box.

(a)

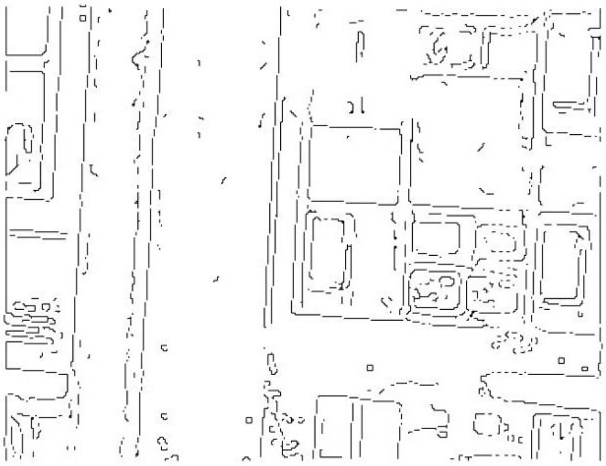

(b)

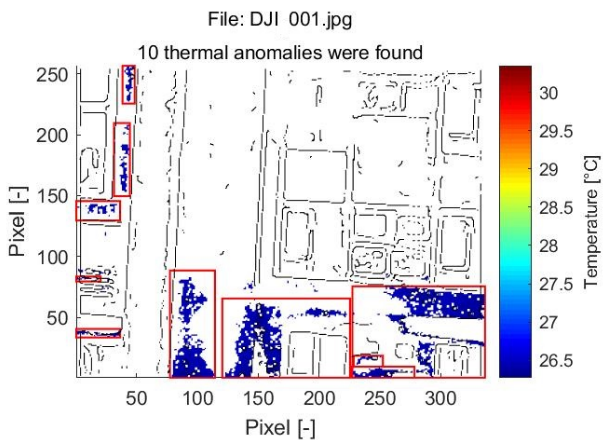

Figure 11. (a) Identification of anomalous edges; and (b) detection of thermal anomalies.

5.4. Micro inspection and anomaly assessment

Micro inspection is performed through an examination of all the detected thermal anomalies. Similar to defect assessment introduced for visual analytics (see Section 4.4), micro inspection is applied to assess the severity of detected anomalies from the macro inspection stage. The severity of thermal anomalies is assessed conforming to the assessment criteria used for stains.

5.5. Post-processing and labelling of anomalies

After the CV model is well built, it can be used for anomaly detection. Since the model is CV-based, all the detection results are reviewed, and final decisions are made. For industrial applications, the algorithm tends to be conservative in terms of anomaly detection; hence, it is more likely to detect false-positives than produce false-negatives. An infrared specialist reviews the outputs of the infrared analytics to assess eventual misdetections and diagnose structural defects causing the thermal anomaly. The false-positives are used for development purposes, and the model is constantly improved inspection after inspection. Figure 12 shows a sample application of infrared analytics through macro inspection and micro inspection on the facade of an RC building.

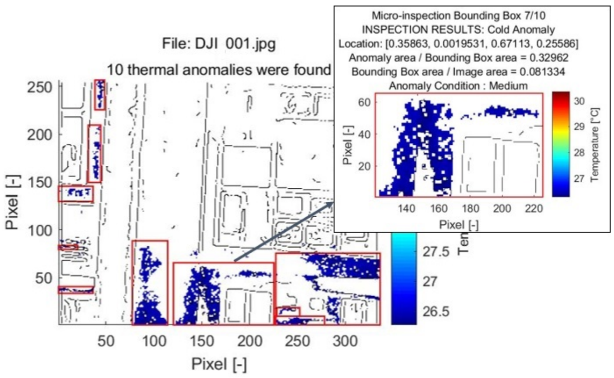

Figure 12. Sample illustration of the application of macro and micro inspection for infrared analytics.

The process of development mentioned above based on database amplification has been undertaken through several inspections. The database has been extended to 4,000+ thermal images, leading to an overall accuracy of 82%. This accuracy is indicative of the model recall, and representative of the percentage of total relevant results correctly classified by the algorithm. Misdetections have been mostly attributed to the inevitable presence of irrelevant objects, reflections on window glass and poorly collected data (not conforming to the specifications listed in Section 3.3).

6. Case study

In Sections 2.1 and 2.2, the differences between qualitative and quantitative approaches for facade inspection have been highlighted. In this section, the industrial application of the proposed AI-powered inspection is compared with the available solutions in the field. As a matter of comparison, a case study of inspection work performed by RaSpect Intelligence Inspection Ltd. is analysed. The inspected site is a facade of one out of 22 individual blocks providing a total of 1,502 domestic units with areas ranging from 434 to 2,000 square feet. The inspected 25-storey facade has a surface area of 27x65 m^2, as displayed in Figure 13(a). The survey flight took place on one single day using four batteries taking visual and thermal photographs. The flight time was 300 minutes, and 1,000+ photographs were captured. The facade was inspected using a Matrice 210RTK (DJI, no date-a) with an X5S visual camera (DJI, no date-b) paired to an XT2 thermal camera (DJI, no date-c). The inspection was conducted using a pre-programmed flight path designed using the Litchi App v2.5.0 (Flylitchi, 2020). The operation crew was composed of one pilot-in-command and one observer/spotter. Since the building is located in a densely populated area, the pilots experienced problems in terms of poor signal reception. Accordingly, the flight path depicted in Figure 2 was adopted with two pre-planned take-off points, from the bottom and top of the building, respectively. The image processing through the described analytics and endorsement of results by a certified professional took four days. The detected defects are labelled under four major categories of inspection outcomes including: cracks, delamination, stains (detected in visual data) and thermal anomalies (detected based on thermal data). The defects are displayed in Figure 13(b). The collected images contain GIS metadata including longitude, latitude and altitude. Such metadata along with the collected images are used for projecting the defects onto the facade. As a result, images are spatially allocated to different portions of the building. All the recognised defects and anomalies are mapped at their location and a comprehensive understanding and evaluation of the status of the facade can be achieved.

(a)

(b)

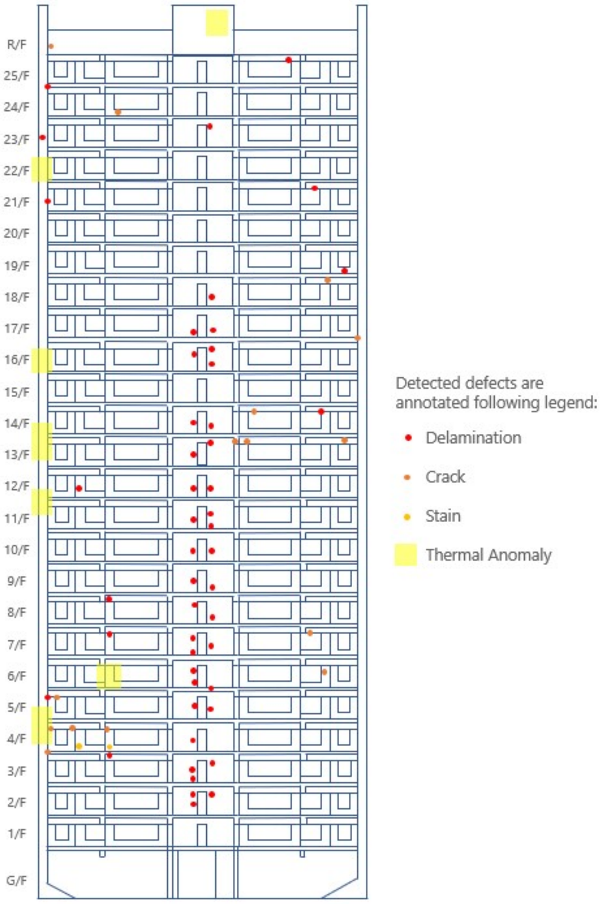

Figure 13. (a) Inspected site; and (b) summary of the inspection results.

With reference to the case study, Table 3 presents a comprehensive comparison between qualitative solutions readily available in the field and the proposed framework for AI-powered inspections.

Table 3. Qualitative vs Quantitative Approaches.

	Qualitative approaches		Quantitative approach
	Facade inspections with scaffoldings	Facade inspections with gondola	AI-powered inspections
Risk	High	Medium/Low	None
Manpower [people/ m^2]	0.011	0.0057	0.0023
Tools & equipment	Planks, cross bars, frame, connecting pins and clams, base plates, safety barriers, level, tape measure, spanners, claw hammer, personal protective equipment	Construction cradle (gondola), suspension mechanism, electric hoists, safety lock, electric control box, steel wire rope, safety rope, counterweights, personal protective equipment	UAV paired with a visual and thermal camera
Automated inspection	✕	✕	✕/✓*
Automated defect detection	✕	✕	✓
End-to-end inspection time / m2 [h]	45+	15+	5
Inspection price / m^2 [HK$]	15.2+	9.5+	5.0
*depending on whether the inspection site is suitable for pre-programmed flight.			

7. Conclusions

This study presents a novel approach for thorough AI-powered inspections of RC buildings. The facade survey was conducted using a UAV paired with a visual and thermal camera. The data were collected following specific recommendations. The collected visual and infrared data were processed using the proposed visual and infrared analytics methods. The developed algorithms enable automated and reliable defect detection based on visual and infrared data from RC facades. The visual analytics algorithm is DL-based, and the model was trained on 18,000+ labelled photographs. The infrared analytics algorithm is CV-based, and it was developed and tested on 4,000+ labelled photographs. Both techniques comprise: (1) macro inspection for defects/thermal anomaly detection based on the collected data and (2) micro inspection for assessment of the severity of defects/thermal anomalies. A case study is included to showcase the industrial application of the proposed method. The following conclusions can be drawn from this study.

- Facade surveys are carried out with UAVs. Drone surveys provide a unique aerial perspective and allow easy access to remote or inaccessible areas without compromising safety. Also, the usage of UAVs allows a very desirable non-destructive and non-contact survey method. Building inspections performed with UAVs exhibit greater accuracy of collected data compared to other inspection methods, whilst drastically reducing the operation time.
- Whilst qualitative approaches for facade inspections are undertaken in an interpretative manner, which may be subjective, the utilisation of a quantitative approach provides a more scalable and effective way of inspecting buildings through automated collection, processing, and analysis of extracted numerical data.
- AI-powered technologies are used for automating and drastically speeding up the inspection process, through DL algorithms for defect detection (including cracks, delamination, and stains) based on visual data and CV algorithms for anomaly detection based on thermal data (due to leakage, debonding and moisture). Regarding the detection of defects, accuracies of 92.5%, 88.3% and 90.6% have been achieved for cracks, delamination and stains, respectively. Regarding thermal anomaly detection, an accuracy of 82% is achieved. The proposed method includes a feature for assessing the severity of all detected defects and thermal anomalies. The industrial applicability of the methodology is showcased, and a comparison has been made between readily available solutions in the field and the novel proposed solution. In general, it was observed that implementation of AI-powered inspections can save up to 67% of the time spent and 52% of the cost in comparison to the best available practice in the field.
- To achieve industrial scale of adoption, the AI model would benefit from a more diverse and segmented dataset composed of more types of building architecture. Achievement of greater variance in the training dataset would allow the model to discriminate between defects better and hence generalise better onto different types of architecture.
- The outcomes of this research work are very promising, and the achieved accuracy and scalability of AI-powered inspection is facilitating its fast adoption in the industry. Through an ever-enlarging database and technological advancements, the authors believe that AI-powered inspections of facades have the potential to overtake the existing leading methodologies.

Acknowledgements

This research work is solely funded by RaSpect Intelligence Inspection Ltd.

Notes on contributors

Dr Michele De Filippo obtained his Ph.D. degree from the Department of Civil Engineering of The Hong Kong University of Science and Technology. He received his M.Sc. from Aalborg University, Denmark with a research internship at the Polytechnic University of Montreal, Canada and his B.Sc. degree at the University of Naples "Federico II" with an exchange at the Polytechnic University of Madrid, Spain. Dr De Filippo received the RPg grant awarded by the Hong Kong Research Grants Council during his Ph.D. studies. His research awards include the HKIE Outstanding Paper Award for Young Engineers/Researchers 2019 from The Hong Kong Institution of Engineers and the Overseas Research Award 2019 from The Hong Kong University of Science and Technology. Dr De Filippo is a former Senior Data Scientist at RaSpect Intelligence Inspection Ltd.

Mr Sasan Asadiabadi is currently a Machine Learning Engineer at RaSpect Intelligence Inspection Ltd. and a Ph.D. candidate and Instructor in the Department of Electrical Engineering at Koc University, Istanbul, Turkey. He received his M.Sc. from Koc University and his B.Sc. from Sharif University of Technology, Tehran, Iran.

Ir Prof J S Kuang is a Professor of Civil Engineering at The Hong Kong University of Science and Technology. His research interests are primarily focused on seismic design and analysis of concrete buildings and structures, and computational modelling in structural engineering. His research awards include the Telford Premium, the T K Hsieh Award and the Magazine of Concrete Research Prize from The Institution of Civil Engineers (ICE), the UK, the HKIE Best Transactions Paper Prize (twice) (previously named the HKIE Transactions Prize) from The Hong Kong Institution of Engineers, and the Grand R&D Award of Structural Excellence Award from The Hong Kong Institution of Engineers (HKIE)-Institution of Structural Engineers (IStructE) Joint Structural Division. He is a Fellow of the HKIE, the ICE and the IStructE.

Prof Dhanada K Mishra has a Ph.D. in Civil Engineering from the University of Michigan, USA. With over 25 years of diverse work experience, he has expertise in concrete structures, non-destructive testing, and structural health monitoring. He has worked both in industry and academia. Prior to his current role as a Technical Director in RaSpect AI, he was a visiting research scholar at The Hong Kong University of Science and Technology. He has over 50 publications in refereed journals and conferences and served as guest editor of *The Indian Concrete Journal*. He is a Fellow of Hong Kong Concrete Institute (HKCI), member of The Institution of Engineers (India), and American Society of Civil Engineers (ASCE).

Mr Harris Sun is the CEO and Founder of RaSpect Intelligence Inspection Ltd. He graduated with an M.Sc. in computer science from The Chinese University of Hong Kong and a B.Sc. in Computer Science and Information System from The University of Hong Kong. He was one of the founding Members of the Innovation Centre of Cathay Pacific Airways. In recent years, he has led RaSpect Intelligence Inspection Ltd. to win multiple start-up competition awards and operations, from academia research projects to private sector projects including: World Summit Awards 2019 (WSA) National Nominee (2019), Winner of Red Herring Asia TOP 100 (2019), HKTDC Entrepreneur Day Start-up Express 2019 Winner (2019), Winner of the TechCrunch China Regional Final (HK) (2018), Winner of Star of Entrepreneurs NanShan Competition (HK) (2018), Award Winner of ShenZhen Innovation and Entrepreneurship (Internet & Mobile Internet) Competition, 2018 (2018), and Award Winner in HKU DreamCatchers 100K (2017).

References

[1] Kwan A and Wong H (2005). *Durability of reinforced concrete structures: theory vs practice*. Proceedings of the Hong Kong Government Standing Committee on Concrete Technology Annual Concrete Seminar. [online]. pp. 1–20. Available at: <http://hdl.handle.net/10722/110796>.

[2] Zhao S (2017). *Old Hong Kong tenement buildings with subdivided flats pose threat as owners neglect repairs*. South China Morning Post. [online] Available at: <https://www.scmp.com/news/hong-kong/economy/article/2099406/old-hong-kong-tenement-buildings-subdivided-flats-pose-threat>. [Accessed on 1 Mar 2020]

[3] Buildings Department (2012). *Mandatory Building Inspection Scheme* [online]. Available at: <https://www.bd.gov.hk/en/safety-inspection/mbis/index.html>.

[4] Mavromatidis L, Dauvergne J, Lunazzi R and Batsale J (2014). First experiments for the diagnosis and thermophysical sampling using pulsed IR thermography from unmanned aerial vehicle (UAV). *Quantitative InfraRed Thermography*.

[5] Harvey M, Rowland J and Luketina K (2016). Drone with Thermal Infrared Camera Provides high resolution georeferenced imagery of the Waikite Geothermal Area, New Zealand. *Journal of Volcanology and Geothermal Research*. 325, pp. 61–69.

[6] Corsi C (2010). History highlights and future trends of infrared sensors. *Journal of Modern Optics*, 57, pp. 1663–1686.

[7] Clark M, Forde M and McCann D (2003). Application of infrared thermography to the non-destructive testing of concrete and masonry bridges. *NDT & E International*, 36(4), pp. 265–275.

[8] Mercuri F, Cicero C, Orazi N, Paoloni S, Marinelli M and Zammit U (2014). Infrared Thermography Applied to the Study of Cultural Heritage. *International Journal of Thermophysics*, 36, pp. 1189-1194.

[9] Barreira E and Freitas V (2007). Evaluation of building materials using infrared thermography. *Construction and Building Materials*, 21, pp. 218–224.

[10] Rakha T and Gorodetsky A (2018). Review of Unmanned Aerial System (UAS) applications in the built environment: Towards automated building inspection procedures using drones. *Automation in Construction*, 93, pp. 252–264.

[11] Flylitchi (2020). Litchi. [online]. Available at: <https://flylitchi.com/>.

[12] Rakha T, Liberty A, Gorodetsky A and Kakillioglu B (2018). Heat Mapping Drones: An Autonomous Computer-Vision-Based Procedure for Building Envelope Inspection Using Unmanned Aerial Systems (UAS). *Technology Architecture and Design*, 2(1), pp. 30–44.

[13] Entrop A and Vasenev A (2017). Infrared drones in the construction industry: Designing a protocol for building thermography procedures. *Energy Procedia*, 132, pp. 63–68.

[14] Pereira FC and Pereira CE (2015). Embedded Image Processing Systems for Automatic Recognition of Cracks using UAVs. *IFAC-PapersOnLine*, 48(10), pp. 16–21. Available at: <http://www.sciencedirect.com/science/article/pii/S2405896315009684>.

[15] Oh J, Jang G, Oh S, Lee J, Yi B, Moon Y, Lee J and Choi Y (2009). Bridge inspection robot system with machine vision. *Automation in Construction*, 18(7), pp. 929–941. Available at: <http://www.sciencedirect.com/science/article/pii/S0926580509000600>.

[16] Khan F, Ellenberg A, Mazzotti M and Kontsos A (2015). *Investigation on Bridge Assessment Using Unmanned Aerial Systems*. Structures Congress 2015 [online]. pp. 404–413. Available at: <https://doi.org/10.1061/9780784479117.035>.

[17] Kim T, Kim H and Cho Y (2021). Product Inspection Methodology via Deep Learning: An Overview. *Sensors (Basel)*. [online]. 21(15), pp.5039. Available at: <https://pubmed.ncbi.nlm.nih.gov/34372276>.

[18] Nwankpa C, Eze S, Ijomah W, Gachagan A and Marshall S (2021). Achieving remanufacturing inspection using deep learning. *Journal of Remanufacturing*, 11, pp. 89–105. Available from: <https://doi.org/10.1007/s13243-020-00093-9>.

[19] Perez H, Tah J and Mosavi A (2019). Deep Learning for Detecting Building Defects Using Convolutional Neural Networks. *Sensors 2019*, 19(16), pp. 3556. Available at: <http://dx.doi.org/10.20944/preprints201908.0068.v1>.

[20] Soto B, Ko P and Prieto S (2021). *ABECIS: an Automated Building Exterior Crack Inspection System using UAVs, Open-Source Deep Learning and Photogrammetry*. Proceedings of the 38th International Symposium on Automation and Robotics in Construction (ISARC) [online]. pp. 637–644. Available at: <https://www.iaarc.org/publications/fulltext/084 ISARC 2021 Paper28.pdf>.

[21] Dutta A and Zisserman A (2019). *The VIA Annotation Software for Images, Audio and Video*. In: Proceedings of the 27th ACM International Conference on Multimedia. [online]. New York: Association for Computing Machinery, pp. 2276-2279. Available at: <https://doi.org/10.1145/3343031.3350535>.

[22] Dutta A, Gupta A and Zissermann A (2016). *VGG Image Annotator (VIA)*.

[23] Kingma DP and Ba J (2014). *Adam: A Method for Stochastic Optimization*.

[24] Chen M, Artières T and Denoyer L (2019). *Unsupervised Object Segmentation by Redrawing*.

[25] Long J, Shelhamer E and Darrell T (2014). *Fully Convolutional Networks for Semantic Segmentation*.

[26] Simonyan K and Zisserman A (2014). *Very Deep Convolutional Networks for Large-Scale Image Recognition*.

[27] Chollet F (2015). *Keras*. GitHub. Available at: <https://github.com/fchollet/keras>.

[28] Abadi M, Agarwal A, Barham P, Brevdo E, Chen Z, Citro C, Corrado GS, Davis A, Dean J, Devin M, Ghemawat S, Goodfellow I, Harp A, Irving G, Isard M, Jia Y, Jozefowicz R, Kaiser L, Kudlur M, Levenberg J, Mane D, Monga R, Moore S, Murray D, Olah C, Schuster M, Shlens J, Steiner B, Sutskever I, Talwar K, Tucker P, Vanhoucke V, Vasudevan V, Viegas F, Vinyals O, Warden P, Wattenberg M, Wicke M, Yu Y and Zheng X (2016). *TensorFlow: Large-Scale Machine Learning on Heterogeneous Distributed Systems*.

[29] Arena A, Delle Piane C and Sarout J (2014). A new computational approach to cracks quantification from 2D image analysis: Application to micro-cracks description in rocks. *Computers & Geosciences*, 66, pp. 106-120

[30] Kim H, Lee J, Ahn E, Cho S, Shin M and Sim SH (2017). Concrete Crack Identification Using a UAV Incorporating Hybrid Image Processing. *Sensors*, 17(9), pp. 2052.

[31] Bauer E, Mota Milhomem P and Aidar L (2018). Evaluating the damage degree of cracking in facades using infrared thermography. *Journal of Civil Structural Health Monitoring*, 8, pp. 517-528..

[32] Shamsudin AM, Fithry Senin S, Hamid R and Yusuf K (2015). Concrete delaminations location and its severity detection by visual inspection and ground penetrating radar. *Journal of Engineering Science and Technology*, Special Issue on 4th International Technical Conference (ITC) 2014, pp. 1-12.

[33] Buildings Department (2012). *Code of Practice for Mandatory Building Inspection Scheme and Mandatory Windows Inspection Scheme*. [online]. Available at: <https://www.bd.gov.hk/doc/en/resources/codes-and-references/code-and-design-manuals/CoP_MBIS_MWISe.pdf>.

[34] Martinez-De Dios JR and Ollero A (2006). *Automatic Detection of Windows Thermal Heat Losses in Buildings Using UAVs*. In: Proceedings of 2006 World Automation Congress. Budapest, Hungary: IEEE, pp. 1–6.

[35] Zhang J, Jung J, Sohn G and Cohen M (2015). *Thermal Infrared Inspection of Roof Insulation Using Unmanned Aerial Vehicles*. ISPRS International Archives of the Photogrammetry, Remote Sensing and Spatial Information Sciences. [online]. XL-1/W4, pp.381-386. Available at: <https://ui.adsabs.harvard.edu/abs/2015ISPAr.XL1..381Z>.

[36] Mauriello ML and Froehlich JE (2014). *Towards Automated Thermal Profiling of Buildings at Scale Using Unmanned Aerial Vehicles and 3D-Reconstruction*. In: Proceedings of 2014 ACM International Joint Conference on Pervasive and Ubiquitous Computing: Adjunct Publication. [online]. New York, NY, USA: Association for Computing Machinery, pp. 119–122. Available at: <https://doi.org/10.1145/2638728.2638731>.

[37] Mauriello ML, Norooz L and Froehlich JE (2015). *Understanding the Role of Thermography in Energy Auditing: Current Practices and the Potential for Automated Solutions*. In: Proceedings of the 33rd Annual ACM Conference on Human Factors in Computing Systems. [online]. New York, NY, USA: Association for Computing Machinery, pp. 1993–2002. Available at: <https://doi.org/10.1145/2702123.2702528>.

[38] De Filippo M, Asadiabadi S, Ko N, and Sun H (2019). *Concept of Computer Vision Based Algorithm for Detecting Thermal Anomalies in Reinforced Concrete Structures*. Proceedings. [online]. 27(1), pp. 8. Available at: <https://doi.org/10.3390/proceedings2019027018>.

[39] Chanda S, Bu G, Guan H, Jo J, Pal U, Loo YC and Blumenstein M (2014). Automatic Bridge Crack Detection – A Texture Analysis-Based Approach. In: El Gayar N et al. (eds). *Artificial Neural Networks in Pattern Recognition*. ANNPR 2014. Lecture Notes in Computer Science. Cham: Springer International Publishing, pp. 193–203.

[40] Canny J (1986). A Computational Approach to Edge Detection. *IEEE Transactions on Pattern Analysis and Machine Intelligence*. [online]. PAMI-8(6), pp. 679-698. Available at: <https://doi.org/10.1109/TPAMI.1986.4767851>.

[41] De Filippo M and Kuang JS (2021). Pseudo-lower bound method for assessing concrete slabs. *Structures and Buildings*. [online]. 174(11), pp.903-919. Available at: <https://doi.org/10.1680/jstbu.18.00130>.

[42] DJI (no date-a). *Matrice 200 Series V2* . [online]. Available at: <https://www.dji.com/uk/matrice-200-series-v2/payloads>. [Accessed on 8 March 2020].

[43] DJI (no date-b). *Zenmuse X5S - DJI Store*. [online]. Available at: <https://store.dji.com/product/zenmuse-x5s?site=brandsite&from=buy_now_bar>. [Accessed on 8 March 2020].

[44] DJI (no date-c). *Zenmuse XT2*. [online]. Available at: <https://www.dji.com/pt/zenmuse-xt2/specs>. [Accessed on 8 March 2020].